Evanescent CHOTs for the optical generation and detection of ultrahigh frequency SAWs

2011 J. Phys.: Conf. Ser. 269 012012

(http://iopscience.iop.org/1742-6596/269/1/012012)

Journal of Physics: Conference Series **269** (2011) 012012 doi:10.1088/1742-6596/269/1/012012

Evanescent CHOTs for the optical generation and detection of ultrahigh frequency SAWs

A. Arca, T. Stratoudaki, R. Smith, M. Clark and M. G. Somekh

Division of Electrical Systems and Optics , Faculty of Engineering, University of Nottingham, Nottingham, NG7 2RD, UK

E-mail: eexaa5@nottingham.ac.uk

Abstract. The use of optical gratings for the generation and detection of ultrahigh frequency narrowband surface acoustic waves is well known. Detection of surface acoustic waves (SAWs) using an optical grating, (without an interferometric set-up) relies on diffraction of light from the grating. Cheap Optical Transducers (CHOTs) for SAWs are optical ultrasonic transducers which are designed to optimise the diffraction from such gratings to yield a local interferometer. They have been demonstrated for typical NonDestructive evaluation (NDE) frequencies (0.5 and 100 MHz). In this paper, we discuss how the CHOTs operate and how their detection mechanism breaks down, when the optical diffraction orders from the grating become evanescent upon moving to multi GHz frequency range. We show that it is possible to design devices with enhanced sensitivity, in this range. This is done by adding a thin "background film" underneath grating fingers, in order to optimise and exploit the interaction between the deformation of the grating and the evanescent fields/ resonances involved in such gratings. The result is a novel operating mechanism, based on an energy balance between the 0-order reflection and resistive heating. These novel transducers are called evanescent wave CHOT (eCHOT). We have used Finite Element Method (FEM) modelling to link the physical displacements caused by the elastic waves with the optical behaviour. We demonstrated that the devices show enhanced sensitivity over a wider range of parameters, than possible with a device designed with conventional CHOT specifications, making the eCHOT an ideal candidate for GHz / nano scale ultrasonics. The eCHOT involves highly resistive thin films and yields thin structures advantageous for ultrahigh frequency ultrasonics. The operating mechanism of the eCHOT suggests that more exotic structures could be built to enhance the sensitivity of these devices.

1. Introduction

The optical detection of ultrahigh frequency (GHz) range surface acoustic waves (SAW) is known to be difficult, since the period of the surface modulation caused by such waves, the SAW wavelength (λ_a) , is small compared to the optical wavelength (λ_o) to cause diffraction of the detection beam. Generation and detection of such waves is important in NonDestructive Testing and Evaluation (NDT&E), when surface breaking cracks are to be analysed.

A key point in producing SAWs of desired frequency and direction is to create periodic disturbances. When utilising a laser, a periodic contrast in the absorption of optical energy, causes the generation of narrowband surface elastic waves. The amplitude of these waves is related to the amount of contrast in the absorption [1]. Usually, generation is achieved by writing a disturbance pattern on a nonabsorbing surface with an absorbing metal, or vice versa and illuminating with a laser pulse [2, 3, 4].

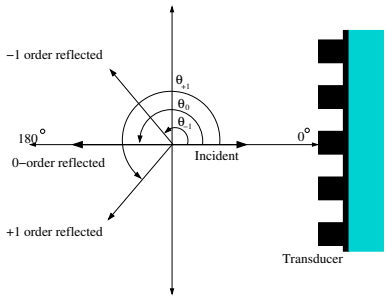

Figure 1. The explanation of the conventions about the farfield observation angles in CHOT and eCHOT simulations. The incident field is considered as a reference at 0° (normal to the surface). The transmitted field is also considered at 0° (on the other side of the sample). All the angles are measured anti-clockwise from this reference direction.

SAWs can be detected by a variety of techniques. These can be classified into interferometric and non-interferometric techniques. Non-interferometric ways include knife-edge, surface-grating, reflectivity methods [5]. Interferometric techniques include optical heterodyning, differential interferometry, velocity or time-delay interferometry [1, 5]. Interferometric systems can have high sensitivity, high bandwidth, and can work on rough surfaces and moving components. In practice, simple interferometry is hard to use and very sensitive, and it will have added complexity in order to deal with problems such as strong sample vibration, air currents and laser pointing instability [5].

Cheap Optical Transducers (CHOTs) for SAWs have been demonstrated for the generation and detection of elastic waves, up to 100 MHz [2], where the acoustic wavelength of interest was bigger than the optical wavelength used. CHOTs can be written on the sample to be analysed as periodically arranged metal stripes, i.e. a grating with period equal to λ_a, for generation and detection. The explanation of the general geometry of the transducers, together with the far field observation angle conventions are shown in figure 1, where the incident field travels from left to right. The generation CHOT (g-CHOT) system works using the above mentioned absorption contrast method. The detection mechanism of the CHOTs (d-CHOTs) does not suffer from the above mentioned sensitivity to outside effects [2]. The operation of the d-CHOTs is based on a local interferometric effect caused by the path difference between the field reflected from the background material and the grating fingers. The transducers are designed and optimised to facilitate the signal via an energy trade mechanism among the reflected optical diffraction orders.

The generation and detection of ultrahigh frequency SAWs have been looked at in the literature by the use of optical gratings [4, 6, 7]. However, the modulation of optical resonances inherent to such suboptical-wavelength transducers due to the interactions with the SAWs has not received much attention. The design of optical transducers by optimising and exploiting this interaction has not been done before.

In this work, we use FEM to investigate and optimise CHOTs for sub-optical wavelength sizes, when all the diffraction orders are evanescent. We find that, once the orders have become evanescent and the energy balance through the diffracted orders is abolished, another energy trade system through resistive heating can be obtained by adjusting the design parameters. This energy trade mechanism relies on the interaction between the optical resonances on the transducer (grating) and the change in transducer geometry due to the deformation caused by the SAW. This deformation causes optical evanescent fields to build up and disappear subsequently around the thin film, modulating the resistive heating in the transducer. This mechanism could be visualised as a thin film moving in and out of a region of concantrated optical field, and

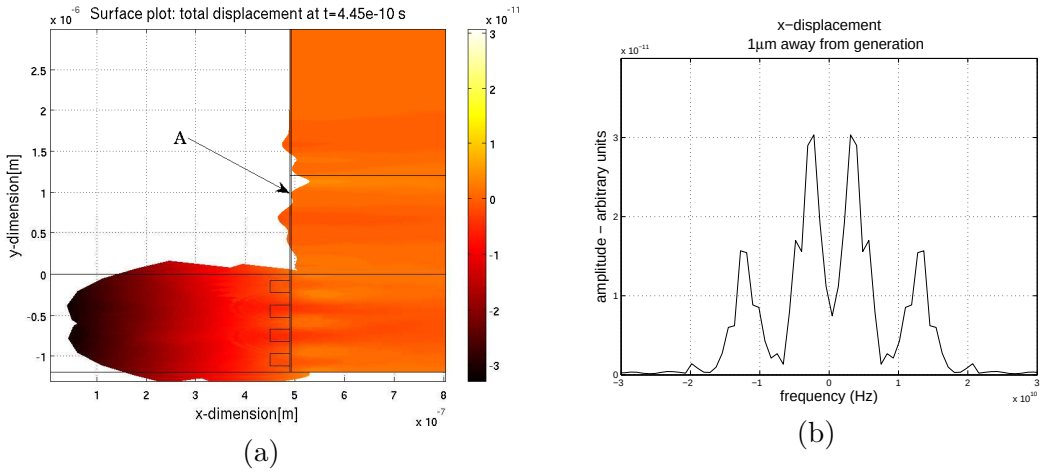

Figure 2. (a) The generation model of the g-eCHOT at time 445 ps (The optical pulse starts around t=0 s.). The surface plot is the total displacement. Additionally, for visualisation purposes, the displacement is also expressed as deformation. The 4 grating fingers are modelled in optical and heat transfer modules, which supply sufficient temperature information around the area. The big bulge in the bottom of the figure, where the transducer is located, represents the high displacement amplitudes due to the heating from the optical source. This model assumes free-space optical wavelength, $\lambda_o = 800$ nm, and acoustic wavelength, $\lambda_a = 300$ nm. Finger thickness is 40 nm and the background film thickness is 2 nm. **(b)** The fourier transform of the x-displacement in the thin film 1 μm away from the generation site (point A on figure 2(a)). Two peaks are seen in the figure. The peak at ≈ 12 GHz is the designed frequency (corresponding to $\lambda_a = 300$ nm). The peak at ≈ 3.1 GHz is a modelling artifact, since 4 fingers are being modelled, it corresponds to $\lambda_a = 1200$ nm.

consequent change in the amount of resistive heating on the thin film. We have optimised this mechanism to design transducers called eCHOTs (evanescent CHOTs) which can generate and detect ultrahigh frequency surface elastic waves with enhanced signal amplitudes, when compared to traditional CHOTs, for a wide range of parameters. The very thin nature of these transducers is also considered to be an advantage due to the small perturbation they pose to the acoustic waves.

2. Model Description

The modelling was done using Finite Element Method [1]. In order to model g-eCHOTs, we have coupled three types of models, optical, heat transfer by conduction, and plane strain. The optical model is used to calculate the resistive heating, which is coupled as a heat source to the "Heat transfer by conduction" model. The heating and the resultant temperature distribution are simulated in the heat transfer model. The temperature distribution in the structure is then coupled to a "Plane strain" model , where the thermal expansion and the resultant displacement are calculated. Hence the effect of optical heating is seen as mechanical displacement.

For d-CHOT and d-eCHOT, a purely optical model is used. The displacement due to the elastic wave is modeled as a sinusoidal deformation of the transducer. The phase of the imposed sinusoid is varied to simulate the passage of a surface acoustic wave. This is referred to as the "SAW phase". The reflected and transmitted optical fields are obtained in the far field as the detection metric.

[1] The implementation of FEM was done with a commercial software Comsol Multiphysics

2.1. Farfield Spectra

The reflected/transmitted farfield spectra are obtained by doing near to farfield transformation using Stratton-Chu Formulations. The Stratton-Chu equation (equation 1) is applied on a circular area on the reflected and/or transmitted side. An appropriate apodisation technique is used to deal with the plane waves which enter and leave the circular boundary undisturbed, so as to simulate a net source enclosed in the circular area.

$$E_p = \frac{jk_n}{4\pi} r_0 \times \int [\mathbf{n} \times \mathbf{E_{ap}} - \eta_n \mathbf{r}_0 \times (\mathbf{n} \times \mathbf{H_{ap}})] \exp(jk_n \mathbf{r}.\mathbf{r}_0) dS \quad (1)$$

Where,
$\mathbf{E_{ap}}$: Electric Field on the aperture(apodised)
$\mathbf{H_{ap}}$: Magnetic Field on the aperture(apodised)
$\mathbf{r}_0$: unit vector pointing from origin to the field point p
$\mathbf{n}$: unit normal to surface S
η_n : impedance of the ambient medium
k_n : wave number in the ambient medium
$\mathbf{r}$: radius vector of the surface S.(not a unit vector)
$\mathbf{E_p}$: calculated far field at point p

3. Results

3.1. g-CHOTs and g-eCHOTs

The heating in the g-CHOT and the g-eCHOT is provided by a laser pulse with pulse length less than the time it takes for an acoustic wave to travel through a grating period. Absorption contrast comes from the thickness dependent absorption constant of Aluminium. In the g-eCHOTs, the pulse length used was approximately 100 fs. The generation mechanism of the g-eCHOT is similar to g-CHOTs, i.e. spatial contrast in resistive heating, thermoelastic generation with a laser pulse. The model used for the generation is shown in figure 2(a). In order to determine the generated acoustic frequency, we have taken the fourier transform of the displacement at point 1 μm away from the generation area (point A in figure 2(a)), which is shown in figure 2(b). In figure 2(b) the fourier transform of the x-displacement(normal component) is shown. There are two distinct peaks corresponding to $\approx$ 12 GHz and $\approx$ 3 GHz. While the former is the frequency of the desired acoustic waves, the latter is a modelling artifact and occurs simply because there are 4 grating fingers in the model. In this model, there is an assumption that the optical source is infinitely long along the periodicity of the grating. However, only four periods are used to represent the above periodicity relationship. Therefore, the periodicity effect due to one finger and four fingers are seen in the models simultaneously. This effect is not physically relevant, hence cannot be seen in an experimental setting.

3.2. d-CHOT

d-CHOTs are reflective gratings which look like metal fingers deposited on a background film. The finger thickness is arranged in order to provide an in situ interferometric effect between the light reflected off the fingers and the background film. When the path difference between these components is arranged to be $\lambda_o/4$, then the modulation of this height due to the passage of an acoustic wave, can cause the maximum change in the 0-order reflected light. For this to occur, the finger height must be around $\lambda_o/8$. As the SAW interacts with the d-CHOTs, the diffracting efficiency of the transducer changes and the energy is redistributed among the diffracted orders. A difference in the intensity of the 0-order reflected light is compensated by the ± 1 diffracted orders. This is shown in figure 3(a). The reflectivity of the transducer(CHOT) is recorded as the signal, while the SAW interacts with the CHOT. The difference between the maximum and

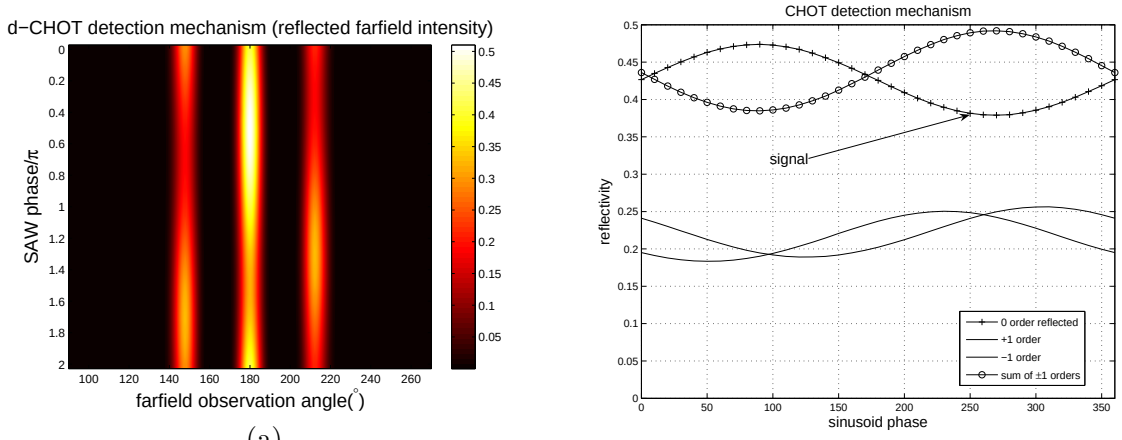

Figure 3. (a) The operation characteristics of the d-CHOT. The reflected farfield intensity spectrum of the d-CHOT mechanism. The 0-order reflected intensity is noted to be the signal (corresponding to farfield angle 180°). The ±1 reflected diffraction orders are seen at farfield observation angles, 147° and 213°, according to the conventions in figure 1. **(b)** The intensity of different propagating components vs the SAW phase (normalised with incident intensity). This plot shows what happens to the intensity of the different field components as the SAW interacts with the d-CHOT, i.e. as the SAW phase changes. It should be noted that none of the diffracted orders are individually 180° out of phase with the 0-order reflected, however, their sum is completely out of phase with the 0-order reflected field, which suggests that the energy difference in the 0-order reflection is compensated equally by the diffracted orders.

the minimum of the recorded reflectivity , i.e. signal, is known to be twice the maximum optical signal amplitude.

When the acoustic wavelength of interest approaches to the optical wavelength used (λ_o), the orders open towards ±90° to eventually become evanescent. When using a substrate with refractive index, $n_g > 1$, some more decrease in the acoustic wavelength can be tolerated, if the background film is thin enough to allow transmission, through the transmitted orders. This is because, transmitted orders can still exist for acoustic wavelengths $\lambda_o/n_g < \lambda_a < \lambda_0$. However, for gratings whose periods are smaller than λ_o/n_g, the operation of this device must be reconsidered, since there will be no more diffracted orders on any side. Once all the diffracted orders become evanescent, only the transmission and absorption can carry away the energy from the signal.

d-CHOTs were designed for acoustic wavelength, $\lambda_a = 1500$ nm and optical wavelength $\lambda_o = 800$ nm, on glass substrates($v \approx 3500$ m/s). The corresponding SAW frequency is ≈ 2 GHz. Figure 3(a) shows intensity of the optical reflection components for this device in the farfield, as the SAW interacts with the transducer. The diffracted orders can be seen at farfield observation angles, -1-order : 147°, 0-order: 180°and +1-order: 213°(The farfield observation angle conventions are given in figure 1). The orders in figure 3(a) correspond to the curves in figure 3(b), as an explanation of the mechanism. As the phase of the sinusoid changes (SAW propagates), the intensity of these diffracted orders change out of phase with the 0-order reflection. The change in 0-order reflected intensity is accounted for by the change in intensity of the ±1 diffracted orders. The ±1-orders sum up to become exactly out of phase with the 0-order reflected wave.

Figure 4(a) shows the operating region for the d-CHOT at different grating finger and background film thickness values. The plotted value is the maximum optical signal amplitude

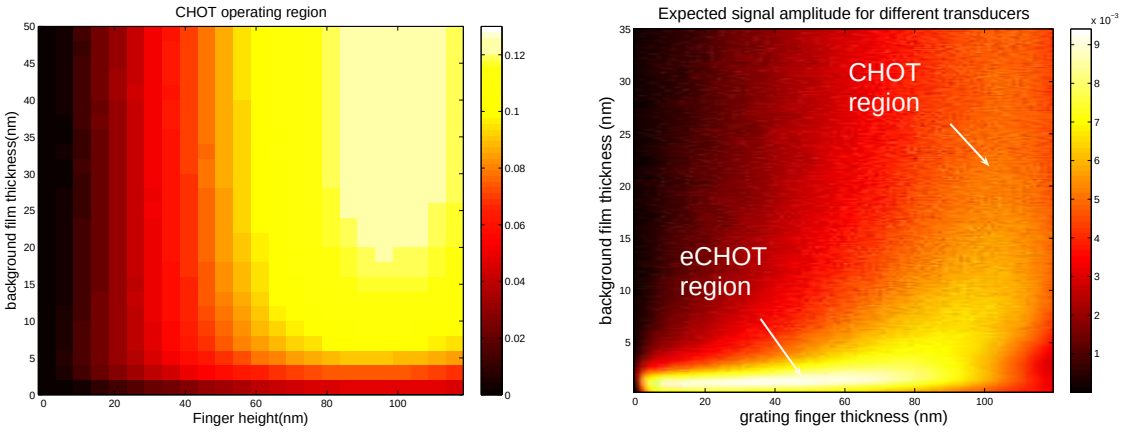

(a) (b)

Figure 4. (a) The effects of finger height and background film thickness on the optical signal amplitude of the CHOT. The plotted quantity is half the maximum change in the reflectivity as the transducer interacts with the SAW. This corresponds to the maximum expected signal amplitude. The specific CHOT device was built from Aluminum, for acoustic frequency 2 GHz (grating period 1.5 μm) and optical wavelength 800 nm. In this simulation the displacement amplitude used was 2 nm. **(b)** The effect of finger height and background film on the operation of the optical detection CHOT transducers. Specific image corresponds to a device designed for λ_a=300 nm. (The period of the grating is 300 nm, corresponding acoustic frequency 12 GHz) The displacement amplitude used was 2 nm. As can be seen, the region that corresponds to a good operating point for (a), i.e. the CHOT region at the long wavelengths, is superceded by a region corresponding to very thin background films and relatively smaller finger heights for smaller wavelengths.

at the given finger height and background thickness value.

The optimum finger height is defined as the finger height at which the change in the observed reflected detection light is found to be the maximum, for a given amplitude of SAW. The optimum finger height is seen to be around 100 nm, where it corresponds to $\lambda_o/8$. The increase in the background film is seen to assist the d-CHOT operation, since the mechanism depends on reflected orders, rather than transmitted and absorbed.

3.3. eCHOT mechanism

The detection mechanism of the eCHOTs is fundamentally different from that of CHOTs. When the light comes in with normal incidence, to the d-eCHOT, it is either reflected, transmitted or absorbed. It cannot be diffracted, since the period of the fingers in the eCHOT is smaller than the optical wavelength. This is seen in figure 5(a). In this figure the reflected farfield spectrum of the eCHOT (finger height 40 nm, background film thickness 2 nm) is plotted as the device interacts with the SAW. The reflected intensity is seen to change with the phase of the sinusoid. As can be seen there are no diffracted orders.

Figure 4(b) shows the effect of the finger height and the background film of a transducer made of Aluminium. As can be seen, there is a region corresponding to finger heights $\lambda_o/8$ which is similar to that of the CHOT criteria, labeled as "CHOT region". Also seen is the part of the image corresponding to low finger and background film thickness, which is labelled as the "eCHOT region". This is the region where the resistive heating is a major contribution to the device operation. As can be seen, the eCHOT area is wide in finger thickness.

The eCHOT operation relies on the interaction between the deformation due to the SAW and

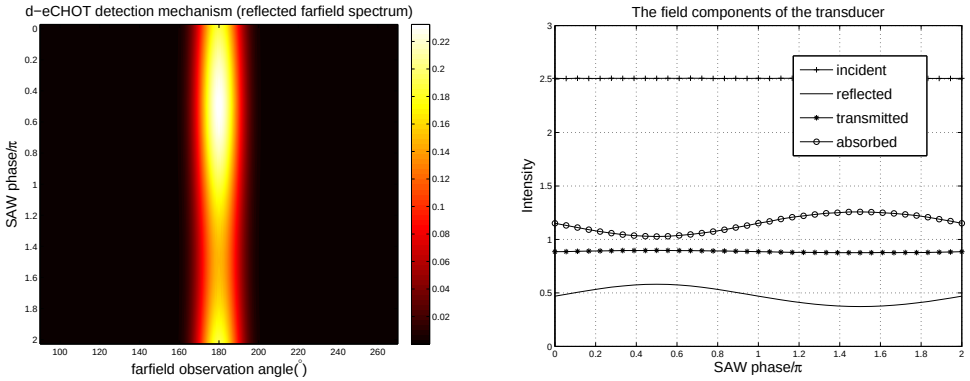

(a) (b)

Figure 5. (a) The reflected farfield spectrum of the d-eCHOT as the phase of the sinusoid is varied. It can be seen that there is no diffracted orders. The only reflected component, namely the 0-order reflection, is seen to vary in intensity as the SAW interacts with the transducer. The considered transducer has 40 nm finger height and 2 nm background film. **(b)** The contribution of various optical components to the energy trade mechanism.These curves are obtained by extracting the field amplitudes from the farfield spectra, followed by the necessary normalisations. The absorption is calculated by subtracting the reflected and transmitted intensity from the incident. It can be seen that as the SAW propagates, the incident intensity is constant, whereas the reflected intensity (the signal) and the absorption are 180° out of phase with each other. The transmitted intensity also has a sinusoidal nature out of phase with the absorption, however, the amplitude of the sinusoid is too small to be visible on this axis. This plot shows that the energy is taken out of the specular reflection via absorption.

the optical evanescent fields/ resonances in the transducer. This is shown in figure 6, where the total field is being plotted at two different instances during the interaction of the SAW with the transducer. In figure 6 it is seen that at certain phases of the SAW, evanescent waves build up on the thin film and at some phases these waves clear off. This modulates the resistive heating in the transducer. This is shown in figure 7, where the resistive heating is being plotted for two distinct instances while the SAW interacts with the transducer. It is seen that the resistive heating in the middle of the thin film is different for the two instances, demonstrating that the transducer works by modulating the resistive heating.

4. Conclusion

We have used FEM modelling to extend the CHOTs concept, to the analysis of suboptical-wavelength-sized gratings in the generation and detection of ultrahigh frequency surface elastic waves. We have seen that by carefully adjusting the design parameters, an increase in the signal amplitude is possible for a wider range of finger thicknesses. We have introduced a new operating mechanism for optical ultrasonic transducers which is based on resistive heating. This mechanism can be used in the design of novel structures involving pointy geometries to confine evanescent fields or lossy surface plasmons.

References

[1] C. B. Scruby and L. E. Drain, *Laser Ultrasonics: Techniques and Applications*. Adam Hilger, 1990.
[2] T. Stratoudaki, J. A. Hernandez, M. Clark, and M. G. Somekh, "Cheap optical transducers(CHOTs) for narrowband ultrasonic applications," *Measurement Science and Technology*, vol. 18, 2007.
[3] M. E. Siemens, Q. Li, M. M. Murnane, H. C. Kapteyn, R. Yang, E. H. Anderson, and K. A. Nelson,

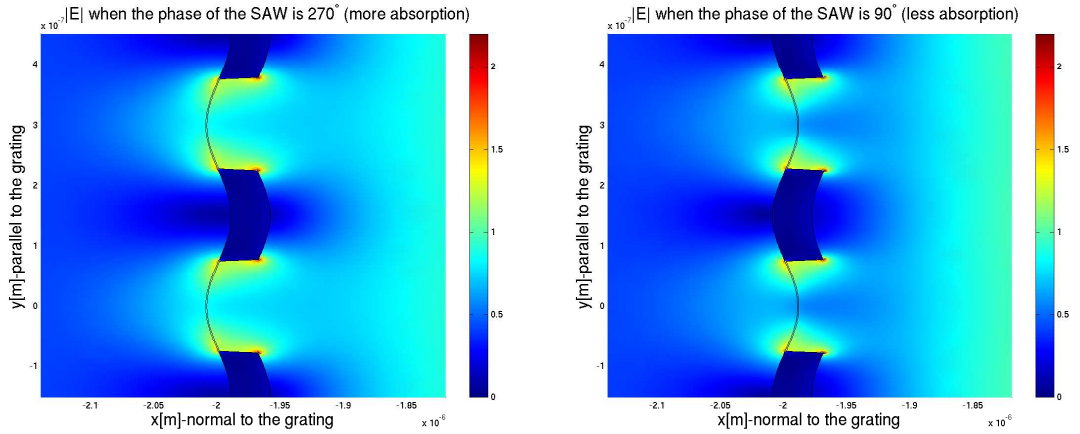

(a) (b)

Figure 6. The demonstration of the effect of evanescent fields in the eCHOT. **(a)**When the phase of the SAW is such that the evanescent field covers the thin film. The film is thus moved into the evanescent field, which increases the absorption. **(b)** When the phase of the SAW is such that the evanescent field does not cover the thin film. The thin film is thus moved out of the evanescent field, in which case the absorption is less.

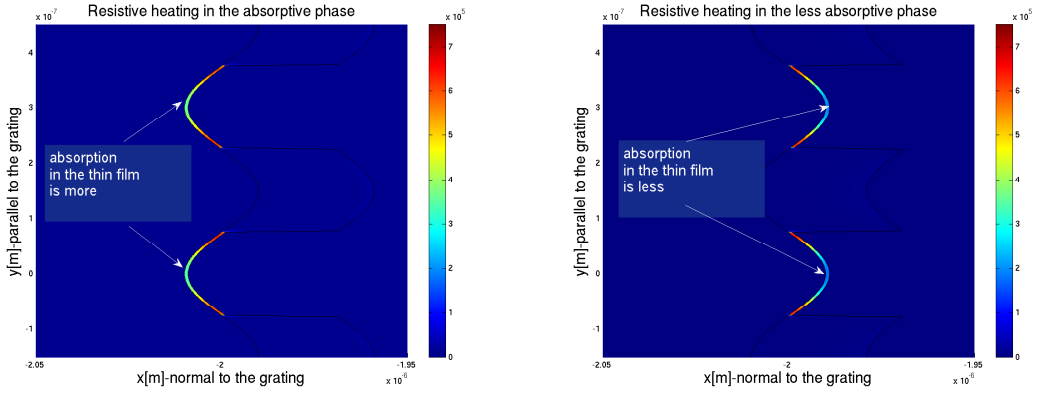

(a) (b)

Figure 7. The demonstration of the modulation of the absorption in the thin film in eCHOT. **(a)** Resistive heating in the thin film in the absorptive phase. (When the phase of the SAW is such that the thin film moves into an evanescent field increasing the absorption.) **(b)** Resistive heating in the thin film, in the less absorptive phase. (When the phase of the SAW is such that the thin film is moved out of the evanescent field yielding less absorption)

"High-frequency surface acoustic wave propagation in nanostructures characterized by coherent extreme ultraviolent beams," *Applied Physics Letters*, vol. 94, 2009.

[4] D. H. Hurley and K. L. Telschow, "Picosecond surface acoustic waves using a suboptical wavelength absorption grating," *Physical Review B*, vol. 66, 2002.

[5] J.-P. Monchalin, "Optical detection of ultrasound," *IEEE Transactions on ultrasonics, ferroelectrics and frequency control*, vol. UFFC-33, no. 5, 1986.

[6] B. Bonello, A. Ajinou, V. Richard, P. Djemia, and S. M. Cherif, "Surface acoustic waves in the GHz range generated by periodically patterned metallic stripes illuminated by an ultrashort laser pulse," *Journal of Acoustic Society of America*, vol. 110, 2001.

[7] D. H. Hurley, "Optical generation and spatially distinct interferometric detection of ultrahigh frequency surface acoustic waves," *Applied Physics Letters*, vol. 88, 2006.